Full-Span Form Panels for Highway Bridges

CLIFFORD O. HAYS, JR., AND JOHN M. LYBAS

Full-span form-panel bridges are bridges constructed of prestressed, precast panels spanning from pier to pier and covered with a composite topping concrete. This paper describes such full-span bridges. Research consists of field investigations, including corings, analytical modeling, laboratory testing, and field testing. Results demonstrate the safety of bridges designed by using the American Association of State Highway and Transportation Officials effective-width formula and describe details thought capable of reducing cracking observed in existing full-span form-panel bridges.

Bridge construction techniques that reduce the amount of on-site concrete forming generally reduce the cost of the structure. Prefabricated prestressed girders have been in common use for approximately 30 years. However, during much of that time it was general practice to cast the deck in the field by using wooden forms between the girders. Precast stay-in-place forms of concrete and steel replaced the wooden forms in recent years and eventually led to the development of precast composite deck panels, which are prestressed slabs that span between bridge girders and support the cast-in-place topping, thereby eliminating most of the field formwork. Past research (1-5) has led to their widespread acceptance and incorporation into American Association of State Highway and Transportation Officials (AASHTO) specifications (6).

For spans of less than 12 m (39.4 ft), however, the most economical bridge would often be a flat slab without girders. The high cost of formwork for such bridges has led to the development of full-span form panels, which are precast panels that are placed side by side, spanning between adjacent piers or abutments and providing stay-in-place forms for a cast-in-place topping. The scheme is shown in Figures 1 and 2. The Florida Department of Transportation (FDOT) has been a pioneer in the use of such panels and based design procedures on the results of research on deck panels that indicated that full composite action could be developed between the panels and assumed that the distribution of live load on the composite section could be safely given by provisions for flat slabs [6, Section 1.3.2 (C)]. Unfortunately, very regular crack patterns have been observed in full-span bridges. This cracking and associated questions about the design assumptions provided the impetus for the work described in this paper.

The study of full-span form panels included several phases:

1. A general field investigation, including corings;
2. Laboratory testing of one-half scale models;
3. Load testing of an actual bridge in the field;
4. Calculation of model and bridge response by using a linearly elastic finite-element model;
5. Calculation of model response to overload by using a nonlinear discrete-element model; and
6. Calculation of shrinkage stresses by using a finite-element model.

The most important aspects of the study are discussed in this paper. The details of the research are provided in the paper by Hays and others (7).

ON-SITE OBSERVATIONS

A total of nine bridges, which were constructed by the full-span slab method, were inspected. All but one were open to traffic. In addition, bridges constructed by competitive construction techniques (cast-in-place deck and girders with either cast-in-place deck or composite deck panels) were inspected.

Of the bridges constructed with full-span form panels, all exhibited essentially the same patterns of cracking. Longitudinal cracks in the deck were observed over almost every longitudinal panel joint and extended for virtually the full length of the bridge. The only significant exceptions were a few of the longitudinal joints closest to the outside of several bridges. These either did not have the crack or the crack ran intermittently over such joints. These outside joints are, of course, not as likely to have traffic loading. However, the one bridge visited prior to being opened to traffic already had several major longitudinal cracks. Thus, it appears that both shrinkage and traffic influence longitudinal cracking.

In addition to the longitudinal cracks, the decks of most, but not all, bridges were cracked transversely over the piers. However, this cracking was often less pronounced than the longitudinal cracking.

It should be noted that longitudinal cracking was also observed in the decks of bridges constructed by other techniques. For bridges that have panels spanning girder to girder, negative-moment cracking over the girders was observed more often than transverse cracking over the panel joints. For other competitive construction techniques, deck cracking was random and did not exhibit distinctive patterns.

BRIDGE DECK CORINGS

Vertical cores 15.2 cm (6 in) in diameter were taken from the decks of several bridges. Figure 3 shows a core taken over a pier that was midway between two longitudinal joints. The negative-moment crack in the cast-in-place topping, which appears approximately vertical on the top of the figure, does not extend to the reinforcing bar. The interface between the end of the form panel and the cast-in-place concrete over the pier is seen as a straight vertical line in the figure, which indicates a lack of bond on that surface.

Figure 1. Typical elevation of one span of bridge.

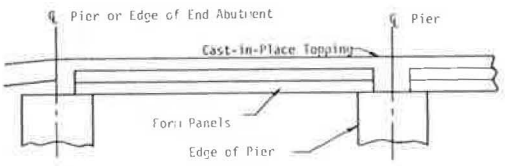

Figure 2. Typical cross section of form-panel bridge.

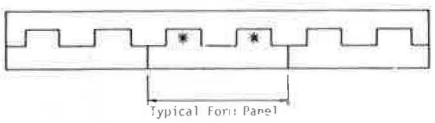

The extensive cracking in the cast-in-place concrete on the right portion of the bottom of Figure 3 occurs where a prestressing strand extends from the precast panel about 5.1 cm (2 in) into the core. During drilling, when one side of the drill was cutting through the prestressing strand, there was no strand on the opposite surface of the core. The resulting stresses caused the cracking around the end of the strand and may have exaggerated the loss of bond along the end of the panel.

Figure 4 shows a core taken above a longitudinal joint at quarter span. The longitudinal crack in the topping is approximately vertical on the top of the figure. A separation between the two form panels is seen in the bottom of the figure. A small amount of concrete and a rope are seen at the joint between the two panels, which indicates that the contractor was using rope to fill a small void between the panels. Both pieces of the panels were separated from the cast-in-place topping during the coring operation. The pieces were reassembled for this figure. However, the interfaces between the form panels and the cast-in-place topping exhibited a clean break that was obviously new and slightly irregular in texture, which indicates reasonable bond.

A number of other corings were obtained in the research, which generally indicated similar patterns of cracking. However, the results are only qualitative due to the high stresses created in drilling the cores.

Figure 3. Core taken at center of panel over pier.

Figure 4. Core taken at quarter span over longitudinal joint.

LABORATORY TESTING

A series of three, one-half scale, two-span continuous bridge deck models were tested in the structural laboratory at the University of Florida. The structures were loaded to failure by concentrated loads that simulated wheel loads. The design load for the slabs was one-half the AASHTO design wheel load of 71 kN (16 kips) and had an impact factor of 1.3.

Test Structures

The configuration of the laboratory tests is shown in Figure 5, and additional information is given in Table 1. The span and thickness of the laboratory models were scaled to one-half the corresponding values for a prototype bridge, while the width of the model was considered to be fully effective in resisting the wheel load. Of course, torsional stresses are much more severe in the model than in a much wider actual bridge deck. Thus, conditions with regard to shear transfer between a loaded and an unloaded panel are more severe in the model than in an actual bridge deck.

The minimum cast-in-place cover allowed by FDOT is 11.4 cm (4.5 in). Thus, the model had a cover of

Figure 5. Laboratory test specimens.

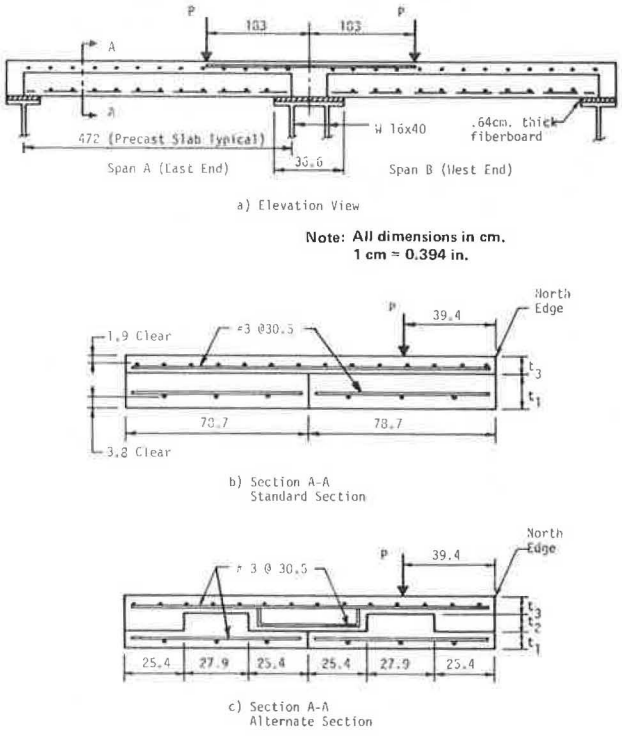

Table 1. Form slab laboratory specimens.

Specimen	Test	Section[a]	Span[a]	t_1[a] (cm)	t_2[a] (cm)	t_3[a] (cm)	No. of Strands in Two Panels[b]	Longitudinal Reinforcement[c] (number of No. 4 bars)
1	1	Standard	A, B	10.2	-	5.7	8	15
2	2	Standard	B	13.3	-	5.7	6	12
		Alternate	A	8.9	4.5	5.7	6	12
3	3, 4	Standard	B	19.1	-	5.7	4	8
		Alternate	A	8.9	10.2	5.7	4	8

Note: 1 cm = 0.394 in.

[a] See Figure 5 for description of section type and span and definitions of t_1, t_2, and t_3.
[b] All were 1.1-cm (0.4375-in) ϕ 1725-MPa (250-ksi) 7-wire strands.
[c] All mild steel reinforcement was grade 60 with a measured average yield stress of 935 MPa (63 ksi).

5.7 cm (2.25 in). Spans in the prototypes are probably most economical in the range of 6-12 m (19.7-39.4 ft). Thus, a laboratory span of 4.6 m (15 ft) was selected.

When the thickness of the slabs is decreased by a factor of one-half, the resulting shear strength is reduced by approximately 50 percent. Thus, the design wheel load for the model was considered to be one-half of that for the prototype. With the load and span each decreased by a factor of one-half, the moments acting at a section of the model are reduced to one-quarter of those for the prototype. It is desirable that the ratio of flexural strength to applied moment for the model be similar to that for the prototype. With the effective depth for the model approximately one-half that of the prototype, the reinforcement areas for the model should be about one-half that of the prototype; they should have the same reinforcement ratios.

In the design of the test structures, analyses were performed for load cases normally considered in the design of the prototype structure. Calculation of stresses under service load were based on elastic theory and were found by adding direct compressive stress due to prestressing, flexural stress due to prestressing, and flexural stress due to applied loads. The precast section was checked for stresses at the time of transfer of the prestress force to the concrete and during construction of the composite section. The composite section was checked for stresses at service traffic loads, which consider live load plus impact. Finally, it was ensured that the flexural strength of the composite section exceeded the moments resulting from the design loads modified by appropriate load factors, as given in Sections 1.2.22, 1.6.9, and 1.6.10 of the AASHTO specifications (6).

The thickness at the edges of the precast slabs was reduced in alternate sections, as indicated in Figure 5 and Table 1, thereby forming an inverted T-shaped slab. Stirrups were placed in the "pocket" that formed between two adjacent slabs (alternate section in Figure 5). It was hoped that this pocket and the stirrups would increase the effective depth of the section across the longitudinal joint and help the bridge act more monolithically. The stirrups were selected to be equal in area to the transverse steel used in the cast-in-place topping. The pocket was dimensioned such that the stirrups would be fully anchored on both sides of the joint.

The transverse reinforcement for the precast panels was the same as that used in the present FDOT specifications and is the minimum requirement for deck panels [6, Section 1.6.26(C)].

The transverse reinforcement for the cast-in-place topping is meant to transfer shear across the longitudinal joint between the precast slabs. Based on the shear-friction concept (8), the shear force is a linear function of the area of steel. Thus, the model that had a load of one-half the load of the prototype had one-half the area of steel used in the prototype.

The major variables in the laboratory tests were the amounts of longitudinal reinforcement in the cast-in-place topping and precast panels, as given in Table 1.

The strengths of the steel reinforcing are given in Table 1. The panels had a design f_c' of 34.5 MPa (5 ksi). However, at the time of testing the specimens, they exhibited an average strength of 41 MPa (6.0 ksi). The cast-in-place topping had a design f_c' of 23.4 MPa (3.4 ksi) and a measured strength of 29 MPa (4.2 ksi).

The precast panels were supplied by a commercial prestressing company. The surface of the slabs was given a broom finish, which appeared quite adequate for bond. Wide flange sections were used as supports for the precast panels (Figure 5); a layer of 0.6-cm (0.25-in) fiberboard was used above and below the supports as a leveling course. The topping was then cast over the present panels and covered with plastic sheets for approximately 48 h after placement. Then the cover and forms were removed and the specimen exposed to the laboratory environment.

For specimens 1 and 2, the topping was cast to form a monolithic unit. However, for specimen 3, a cold joint in the topping was constructed over the longitudinal joint where the precast slabs meet, thus providing a potential cracking plane.

Loading and Instrumentation

The test structures were loaded vertically by one hydraulic jack in each span (see Figures 5 and 6). The distribution of the load was accomplished through 20.3x30.5-cm (8x12-in) bearing plates with rounded corners, which provided an average pressure of 570 kPa (83 psi) under the 35.6-kN (8-kip) design wheel load.

Vertical deflections were measured at the positions shown in Figure 6 by using linear variable differential transformers (LVDTs) and mechanical dial gages. Note that the dial gages were used to measure the settlement of the fiberboard layer in the supports. The correction of the LVDT readings for these base deflections is illustrated in Figure 7. Note that the LVDT readings were with respect to the very slightly cambered position of the specimens prior to the application of the test load. The distance b', which is the part of the deflection due to the translation and rotation of the chord, was subtracted for the total deflection b to obtain the relative (or chord) deflection.

Behavior of Test Structures

Tests 1-3 corresponded to test structures 1-3. The

Figure 6. Location of gages for laboratory tests.

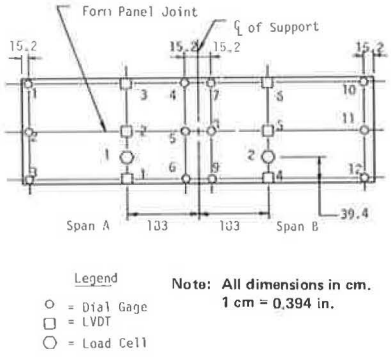

Figure 7. Corrections for chord deflections.

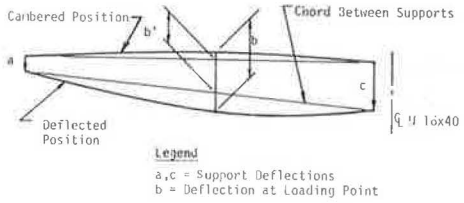

Figure 8. Variation of load with deflection of one span of each laboratory test.

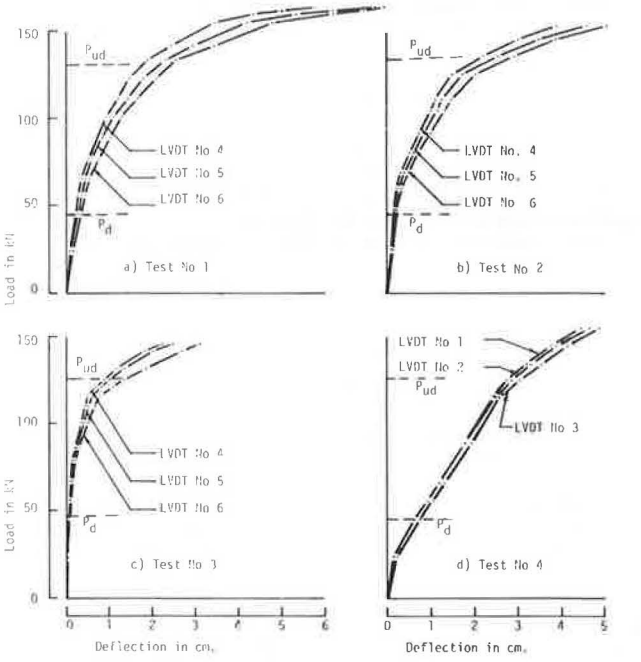

Note: LVDT numbers correspond to Figure 6.
1 cm = 0.394 in, 1 kN = 0.225 kip.

loads in the two spans were constrained to be approximately equal. However, one span failed first in all cases. Test 4 was a retest of the unfailed span of structure 3. For each test, Figure 8 shows the variation of load with deflection for the span that eventually failed. The AASHTO design load P_d and the ultimate flexural strength P_{ud} of the span, as obtained from Sections 1.6.9 and 1.6.10 of the AASHTO specifications (6), are indicated in the plots.

For the first two load increments, which were near the design load, the specimen responded linearly with either no observed cracking or some very minor hairline cracking over the supports that are associated with negative moment. At between 1.5 and 2 times the design load, positive-moment cracks opened in the bottom of the loaded (north) panel and in some cases the unloaded (south) panel. In all cases, positive-moment cracks extended across both the loaded and unloaded panels prior to failure. Before positive-moment cracking was observed, negative-moment cracks were very extensive and extended over the full width of the specimen.

After being extensively cracked, the specimens still increased in load capacity and exhibited good ductility until an inclined crack was observed between the load and the interior support on the edge of the loaded panel. Then, after exceeding the calculated structure strength, a final punching shear failure occurred. Except for the third test, which had a cold joint above the longitudinal joint between the form panels, no longitudinal cracking was observed except in conjunction with the final failure.

In contrast to the other test structures, structure 3 (test 3) had a cold joint in the topping concrete over the longitudinal joint between the precast form panels. For this structure, a longitudinal crack developed in the cold joint. The crack first appeared near the loading plate at a load of about twice the design loading. At failure, the longitudinal crack ran essentially the full length of span B but did not extend into span A (span A had the alternate cross section shown in Figure 5). Final punching failure occurred at a load about 5 percent less than that for test 2 but well above the predicted ultimate strength.

The punching failure for test 3 is shown in Figure 9. The failure mechanism for other test structures was quite similar. In Figure 9, the diagonal crack on the edge of the slab is inclined from the horizontal about 45°, as in a typical beam shear failure. However, where the crack becomes longitudinal in the neighborhood of the load, the surface of the crack forms a very shallow angle with the top surface of the slab and, even where it intersects the longitudinal cold joint in the topping, it does not generally extend below the topping concrete. The failure mechanism appears to be a combination of beam and punching shear and is perhaps aggravated by the loss of shear transfer across the longitudinal cold joint in the topping that is associated with the intersection of the punching crack with that joint.

The good bond between the cast-in-place topping and the form slabs is obvious in that no separation is visible at the 45° shear crack on the side of the slab.

The punching failure was quite sudden and would be cause for concern if not for several reasons. First, failure in all tests occurred after the predicted structure strength had been exceeded considerably and good ductibility was exhibited. Second, torsional response (which greatly increases the shear stresses around the longitudinal joint) is much more severe in the laboratory model than in prototype bridges.

FIELD TESTING

The prototype on which the field-testing phase of this project was performed was the Lloyd Creek Bridge, an eight-span bridge where all the spans are approximately 7 m (23 ft) in length. The precast panels are a constant 17.8 cm (7 in) thick and have a 14-cm (5.5-in) layer of concrete used as the topping.

Figure 9. Shear crack in laboratory specimen.

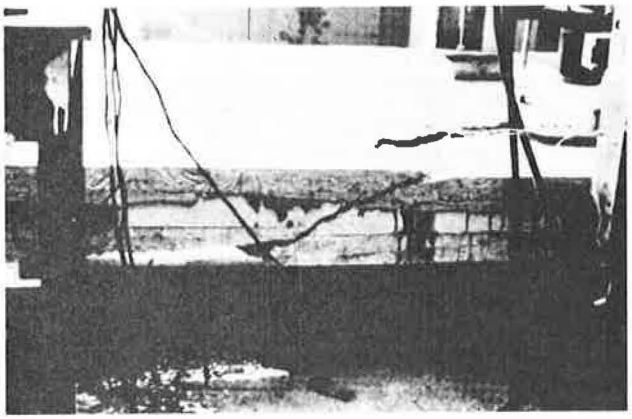

Figure 10. Hydraulic loading for field test.

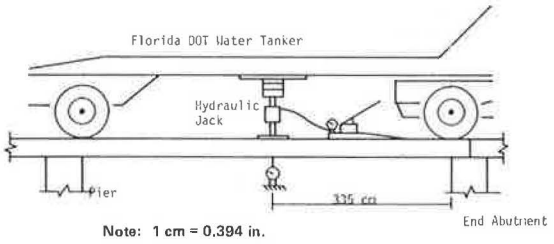

Note: 1 cm = 0.394 in.

Figure 11. Location of gages for field tests.

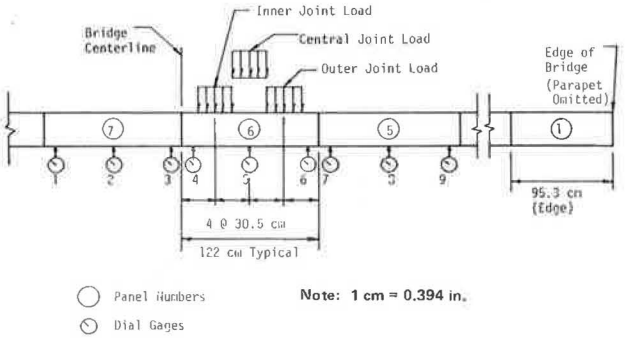

Note: 1 cm = 0.394 in.

Hydraulic Loading

In the first eight tests, load was applied by jacking against the underside of an FDOT tank trailer, as shown in Figure 10. The distance between the wheels of the tractor and trailer was such that two sets of the wheels rested almost completely on the supports. All other wheels were either off the bridge or raised above the slab. With the truck in this position, the load in the piers was virtually constant as the load in the jack varied; thus, support settlement was not a problem. The position of loading relative to the cross section of the bridge is shown in Figure 11. The bridge has 12 panels across a section; panels 1, 5, 6, and 7 are shown in Figure 11. The load was applied to panel 6, which is 3.35 m (11 ft) from the end abutment (Figure 10), at one of three positions in the cross section (the panel centerline) and at 30.5 cm (12 in) from either edge of the panel. These positions will be denoted central load, inner joint load, and outer joint load, as noted in Figure 11.

The loads were applied in increments of 35.6 kN (8 kips) to a maximum load of 142.4 kN (32 kips), roughly 1.5 times the design wheel load, including impact. Distribution of load was obtained by using one of two different bearing plates. The primary one was a 30.5-cm (12-in) diameter plate provided by FDOT. This gave a pressure under the 142.4-kN load of 1950 kPa (283 psi), which was thought to be high. To better simulate a wheel load, several tests were also run with a larger bearing plate. This wheel plate had an elongated central portion and semicircular ends, which followed recommendations by Yoder (9). This plate produced a pressure of 1000 kPa (145 psi) under the 142.4-kN load. Results from using the two different plates were very similar.

Deflection Measurements

By using mechanical dial gages, deflections relative to the ground were measured at the cross section of the application of load and at the positions in the section shown in Figure 11. The positions were either at a panel centerline or 3.8 cm (1.5 in) from a panel edge.

Test Procedure

At the start of each test, the truck was positioned as shown in Figure 10. Deflections were recorded with no load in the hydraulic jack and then after the application of each load increment. The load was then returned to zero and a final set of deflection readings were taken. In general, the initial and final deflection readings were not equal. Because the structure was known to behave elastically under the magnitude of loading applied, the difference was attributed to temperature variations. The deflections for each load increment were adjusted to account for this difference.

Tank-Trailer Loading

In addition to the load test under incremented hydraulic loading, the deflections of the bridge were also measured under the load of the truck itself. The truck was positioned with the rear axle of the trailer directly above the line of dial gages in the end span and the other axles off the bridge. The axle load applied to the span was 115.7 kN (26 kips).

Calculation of Deflections

The internal moments and deflections for the bridge were computed by using a finite-element model (10). The element used was a plate-bending rectangle with three degrees of freedom, vertical deflection, and two rotations at each node. The material was assumed to behave linearly elastically; the thickness of the elements was chosen such that the flexural section stiffness per unit length for the model and for the prototype was equal. In computing the stiffness of the prototype's composite section, the elastic moduli for the various concretes were assumed to be given by ACI 318-77 (8). Computations were performed by using one span that was seven form panels across. The assumption was that, in the actual bridge, form panels far from load would not contribute to the structure response. The continuity of the bridge deck over interior supports was modeled by using vertical and rotational springs. Details on the finite-element model are given in Hays and others (7).

Discussion of Measured and Computed Deflections

The variation of measured vertical displacement across a section of the bridge is shown in Figure 12 for three of the eight hydraulic loading tests for a load of 142.4 kN (32 kips). Computed displacements are shown on the same set of axes. Figure 12 represents results that were typical for the study; the balance of the results are presented in Hays and others (7).

The results shown in Figure 12 are for the three load tests with an outer joint load and a circular bearing plate. Of the two finite-element models considered, B1 was considered a reduced panel thickness for a distance h at the longitudinal joints, as shown in Figure 12, while B2 was considered a uniform thickness.

The measured deflections indicate various amounts of shearing deformations at the longitudinal joints. Considering all eight field tests, test 5 (included in Figure 12) produced the largest differential deflection across the longitudinal joint. This, however, was only 0.013 cm (0.005 in)--approximately 6 percent of the deflection at that point. Deflections measured due to the actual axle load indicated even less differential deflection at the longitudinal joints than those due to the loading through the single bearing plate.

Comparison of the computed and measured results in Figure 12 indicates that the model with a uniform deck thickness (B1) better simulates the overall magnitude of bridge deck deflection. However, the model with reduced thickness at the longitudinal joints (B2) is much better at simulating the shape of the variation of deflection across the section.

The fact that model B2 overpredicted the magnitudes of deflections indicated that it had a lower stiffness than the actual bridge. This may be attributed primarily to two factors. First, the elastic modulus of concrete for the model was computed by using the nominal or design value of f_c'. The actual value of E is probably larger than the value so computed. Second, the model considered only the loaded panel and three panels on either side, thereby neglecting a total of five outer panels of the bridge. Thus, using the reduced-thickness model along with a more accurate modulus of elasticity would be expected to give quite good deflection profiles.

Computed Moment Distributions

Longitudinal bending moments in the bridge deck were computed by using the finite-element model. Figure 13 shows the distribution of these moments over the cross section of the span where the loads were applied in the field tests, i.e., the same section considered for deflections in Figure 12. Results are shown [for a load of 142.4 kN (32 kips)] for two previously defined load positions and two variations of the model.

As shown in Figure 13, the model that considers reduced deck thickness at the longitudinal joints produced discontinuities in moment at the abrupt changes in deck thickness, the moments in the reduced-thickness region being approximately 2 percent of the adjacent moments. Furthermore, the maximum moments for the longitudinal joint model were 26-33 percent greater than those for the uniform-thickness model. The moments at edges of the finite-element model were less than 30 percent of those in the loaded panel, which indicated that the finite-element model (7 panels in width) was a reasonable representation of the actual bridge, which was 12 panels in width.

Finally, the computed longitudinal moments have implications for the AASHTO effective-width formula. Consider two wheel loads 6-ft center to center at a particular cross section of the span, as would be the case for the two tires on one axle of a trailer. Referring to Figure 14, if the outer joint load is one of the two wheel loads, the other load will be centered at point A. The maximum moment in the section will occur near the outer joint load and will be the sum of the moments caused by each of the two loads. By Maxwell's law, the moment at the outer joint load due to the load at A is equal to the moment at A due to the outer joint load, which

Figure 12. Deflections across transverse section.

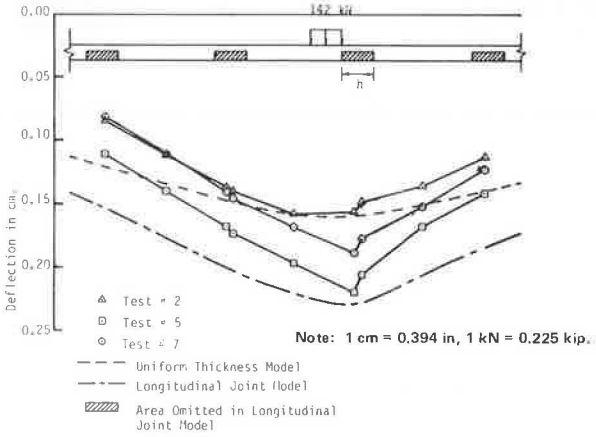

Figure 13. Longitudinal moments across transverse section at applied load.

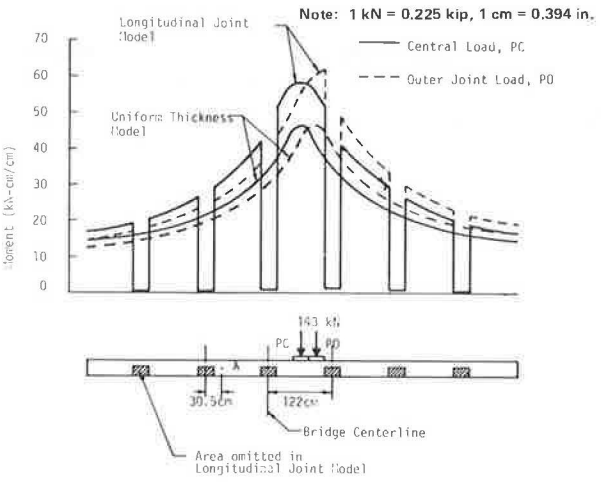

Figure 14. Proposed detail of full-span form panels.

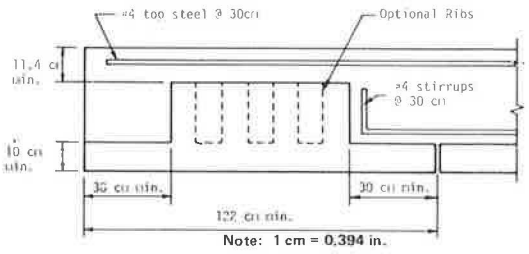

(from Figure 14) is approximately 26 kN-cm/cm (5.8 kip-in/in). The maximum moment due to the outer joint load is approximately 62 kN-cm/cm (13.9 kip-in/in). The sum is 88 kN-cm/cm (19.8 kip-in/in). Considering the AASHTO effective-width formula, along with a linearly elastic beam analysis for a single 142.4-kN (32-kip) load positioned along the span as for the finite-element analysis, the resulting maximum longitudinal moment at the cross section of the load is 125.9 kN-cm/cm (28.3 kip-in/in). Hence, the finite-element model implies that the AASHTO effective-width formula is conservative. A similar comparison for negative moments at a support (7) indicates even more conservatism in the AASHTO formula.

CONCLUSIONS AND DESIGN RECOMMENDATIONS

The following conclusions and practical recommendations were derived from the study described in this paper.

1. With reasonable surface treatment of the precast panels, loss of bond between the panels and the cast-in-place topping should not be a problem. A broom finish of the panels, along with wetting prior to placing the topping concrete, should result in excellent bond. A minimal amount of shear reinforcement would provide added assurance.
2. Shrinkage stresses induced in the topping concrete during curing are likely to be large enough to cause cracking, especially longitudinal cracking over the longitudinal joints between form panels (7).
3. It appears that the AASHTO effective-width formula is adequate for determining the design longitudinal moments due to live load. However, because there is some increase in peak elastic moment compared with a poured-in-place solid slab, it is recommended that a minimum panel width of 122 cm (48 in) be established. Panels with smaller widths that are designed by the effective-width formula would have adequate ultimate strength. However, such panels might be highly stressed under moderate overload.
4. It appears that the minimum transverse reinforcement in the topping of No. 4 bars at 30-cm (12-in) center-to-center, along with the minimum topping thickness of 11.4 cm (4.5 in), will provide adequate shear transfer over the longitudinal joint between adjacent panels. However, the joint detail shown in Figure 14 should provide improved performance in regard to longitudinal cracking and load transfer. The figure depicts the cross section of one form panel and part of the adjacent panel. The thickness of each form panel is reduced adjacent to the joint, thereby providing a larger thickness of cast-in-place topping over the longitudinal joint. Stirrups should then be placed in the topping over the joint to further improve load transfer. A reduced thickness of approximately 10 cm (4 in) should be sufficient to resist stresses in the precast panel yet provide improved joint behavior. The 30-cm width of the reduced-thickness portion is sufficient for anchorage of No. 4 stirrups at 30-cm center-to-center and allows tolerance on placing the stirrups in the pocket. The center portion of the panel could be either ribbed, as shown by dashed lines, or flat.
5. The present detail at the piers and end abutments is similar to that in Figure 5, except that the flexible bearing pads extend only under the precast panels. An improved detail that has more positive transfer of shear from panels to supports is needed to reduce deformation and cracking in the region of the support and to increase the overall stiffness of the bridge. This could be accomplished by placing horizontal shear keys in the ends of the precast panels or by providing for some direct bearing of the panels on cast-in-place concrete over the supports.
6. Reinforcement for positive transverse moment over the piers should be provided in accordance with Obranic (10). However, it is possible that with the increased shear transfer on the ends of the panel, some minor positive-moment cracking over the piers would not be too detrimental.

In summary, the full-span form-panel bridges visited during field investigations are quite safe and, based on the findings of this research, are in no danger of failure. However, one or two of the more highly traveled bridges might experience some maintenance problems in the future due to the cracking in the deck. Future bridges built with the recommended details should be equivalent to conventional, more expensive cast-in-place flat slabs not only in strength, but also in serviceability.

ACKNOWLEDGMENT

We would like to acknowledge FDOT for its financial support of the research on which this paper is based. Also, two graduate students--R.L. Cox, Jr., and G.O. Obranic, Jr.--worked long and diligently on the research and are owed a special thanks.

The opinions, findings, and conclusions are ours and not necessarily those of FDOT.

REFERENCES

1. R.M. Barnoff and D.E. Rainey. Laboratory Tests for Prestressed Concrete Deck Panels and Deck Plank Assemblies. Pennsylvania Transportation Institute, Pennsylvania State Univ., University Park, June 1974.
2. E. Buth, H.L. Furr, and H.L. Jones. Evaluation of a Prestressed Panel, Cast-in-Place Concrete Bridge. Texas Transportation Institute, Texas A&M Univ., College Station, Sept. 1972.
3. R.W. Kluge and H.A. Sawyer. Interacting Pretensioned Concrete Form Panels for Bridge Decks. Engineering and Industrial Experimentation Station, Department of Civil Engineering, Univ. of Florida, Gainesville, Final Rept. D610-635F, 1974.
4. R.W. Kluge and H.A. Sawyer. Interacting Pretensioned Concrete Form Panels for Bridge Decks. PCI Journal, Vol. 20, No. 3, May/June 1975, p. 34.
5. H.A. Sawyer and J.-B. Dansby. Transverse Reinforcement in Pretensioned Concrete Form Panels for Bridge Decks. Engineering and Industrial Experimentation Station, Department of Civil Engineering, Univ. of Florida, Gainesville, Progress Rept. D635P, 1974.
6. Standard Specifications for Highway Bridges, 12th ed. AASHTO, Washington, DC, 1977.
7. C.O. Hays, R.L. Cox, and G.O. Obranic. Full Span Form Panels for Short Span Highway Bridges. Engineering and Industrial Experimentation Station, Department of Civil Engineering, Univ. of Florida, Gainesville, Final Rept. U17F, Sept. 1980.
8. Building Code Requirements for Reinforced Concrete (ACI 318-77). American Concrete Institute, Detroit, 1977.
9. E.J. Yoder. Principles of Pavement Design. Wiley, New York, 1959.
10. G.O. Obranic. Analysis of Composite Bridge Decks with Pretensioned Concrete Form Panels. Univ. of Florida, Gainesville, Master of Engineering thesis, 1980.

Publication of this paper sponsored by Committee on Construction of Bridges and Structures.